

# World Stress Map Database as a Resource for Rock Mechanics and Rock Engineering

Arno Zang · Ove Stephansson ·  
Oliver Heidbach · Silke Janouschkowetz

Received: 5 May 2011 / Accepted: 3 March 2012 / Published online: 27 March 2012  
© Springer Science+Business Media B.V. 2012

**Abstract** Knowledge of the in situ stress state is of key importance for rock engineering. We inform the reader about the World Stress Map (WSM) database and its application to rock mechanics and rock engineering purpose, and in particular the orientation of maximum horizontal stress. We discuss the WSM and the quality ranking system of stress orientation data. We show one example of discrete-measured and computed-smoothed stress orientations from central and northern Europe with respect to relative plate velocity trajectories. We give first insights into ongoing development of a second, more Quantitative World Stress Map database which compiles globally rock-type specific stress magnitudes versus depth. We discuss the vertical stress component, and the lateral stress coefficient versus depth for different rock types. We display stress magnitudes in 2D and 3D stress space, and investigate stress ratios in relation to depth, lithology and tectonic faulting regime.

**Keywords** Lithologic stress magnitudes · Quality ranking system · Quantitative World Stress Map (Q-WSM) · Rock engineering · Stress orientation · Stress space · World Stress Map (WSM)

## 1 Introduction

Rock stress is important in geotechnical applications (Hudson and Harrison 2000) and in solid Earth sciences (Zang and Stephansson 2010). Gravity as well as long-term geological processes like plate tectonics are driven by mechanisms that generate stresses in the Earth's crust. These stresses induce deformation as we extract raw materials from the crust and deposit human altered materials into the crust in boreholes, mines and underground openings. Management of underground structures take into account the existing stress either to take advantage of the state of stress, or at least to minimize the effects of man-made stress changes. Knowledge of the present-day stress field is of interest, when civil engineers are planning and constructing underground excavations and carrying out safety analyses of tunnels, mining engineers are planning and exploiting underground mines, and engineers are extracting oil and gas from a petroleum field, or heat from a geothermal field. Regional stresses are of major interest when tectonic deformations near faults and related earthquake hazard need to be quantified (Hergert and Heidbach 2011). World-wide stress pattern are important when mantle flow models and plate velocities

---

A. Zang (✉) · O. Stephansson · O. Heidbach  
Department 2: Physics of the Earth, Section 2.6 Seismic Hazard and Stress Field, German Research Center for Geosciences (GFZ), Telegrafenberg, 14473 Potsdam, Germany  
e-mail: zang@gfz-potsdam.de

S. Janouschkowetz  
R+V Versicherung AG, Reinsurance, Underwriting Support, Leipziger Straße 35, 65191 Wiesbaden, Germany

are discussed in a global reference frame (Steinberger and Torsvik 2008). Among the more notable reviews of Earth stresses are those of Hast (1969), Herget (1974), Haimson (1975), McGarr and Gay (1978), Rummel (1979, 1986, 2005), Zoback and Zoback (1980), Gough and Gough (1987), Hickman (1991), Zoback (1992, 2007), Engelder (1993), and Amadei and Stephansson (1997). Since there is no internationally agreed terminology for words describing the state of stress in a rock mass (Hudson et al. 2003), for rock stress terms used throughout this paper (e.g., in situ, primary, virgin, pre-mining, natural, secondary, man-made, mining induced, perturbed, local, regional, plate-tectonic, first, second, third-order, initial stresses), we refer to our recently suggested and published rock stress terminology (Zang and Stephansson 2010).

Voight (1969) hypothesized that in situ stress measurements may provide an important constraint for models that investigate the large scale tectonic processes, and that the origin of the compressive stresses within the North American plate is generated by plate boundary forces that drive plate tectonics. Following his hypothesis, Sbar and Sykes (1973) compiled 39 data records of stress information from overcoring, hydrofracs and earthquake focal mechanism solutions in Eastern North America as well as postglacial geological features. They found that the estimated orientation of maximum horizontal stress ( $S_H$ ) is constant over large areas. From this observation they conclude that their findings support Voight's hypothesis and argue that stress measurements are of key importance in understanding global plate tectonics. Sykes and Sbar (1973) determined the earthquake focal mechanisms of 69 intra-plate events and found that in most areas the horizontal stresses are larger than the overburden. These results are confirmed by a comprehensive global compilation of 116 in situ stress magnitude measurements and 59 stress orientations of Ranalli and Chandler (1975). They concluded that (1) in crystalline rock, the horizontal stress magnitudes (minimum  $S_h$ , maximum  $S_H$ ) are usually higher than the vertical stress magnitude ( $S_{h,H} > S_V$ ), (2) in sedimentary basins, the situation is reverse ( $S_{h,H} < S_V$ ), and (3) in general, the stress field is anisotropic, i.e., stress magnitudes are not equal ( $S_h \neq S_H \neq S_V$ ). However, they also point out that the number of stress data records is not sufficient to allow a construction of the contemporary tectonic stress field and that local stress perturbations, e.g., due to the effect of topography on shallow measurements,

potentially introduce an uncertainty on stress data with respect to the interpretation in a regional context.

After the findings of Bell and Gough (1979) that borehole breakouts can be used as a proxy for the  $S_H$  orientation, Zoback and Zoback (1980) compiled 236 data records from various stress indicators for the United States. They conclude that the  $S_H$  orientation is constant for large areas with up to 2000 km in dimension. This compilation was the starting point of global compilation of stress data as a joint effort of several research groups world wide—the World Stress Map (WSM) project has been launched (Zoback et al. 1989; Zoback 1992; Sperner et al. 2003; Heidbach et al. 2007, 2010). So far, the WSM stress compilations focus on stress orientations, the magnitudes of in situ stresses being neglected.

In this paper we briefly review the purpose, history and milestones of the WSM project. We also give a brief overview of the origin, quality and spatial distribution of the 21,750 stress data records that have been compiled in the WSM database release 2008. In addition, we present the first results on our new initiative to globally compile in situ stress magnitude measurements in a second database. This so-called Q-WSM (Quantitative WSM) database accounts for lithologic stress magnitudes, and is important in particular, for geomechanical reservoir modelling and rock engineering applications. Rock-type-specific in situ stress magnitudes are the key (1) to assess optimal drilling path ways with prediction of fracture propagation in hydraulic stimulation (Hopkins 1997; Fuchs and Müller 2001), (2) to improve wellbore stability analysis (Aadnoy and Hansen 2005), (3) to constrain initial conditions of 3D reservoir models and the effect of man-made stress perturbations (Henk 2008; Hergert and Heidbach 2011), and (4) to compute slip tendency, i.e., the fracture potential of pre-existing faults (Morris et al. 1996; Connolly and Cosgrove 1999; Moeck and Backers 2011).

## 2 World Stress Map Project

In this chapter, a brief history of the World Stress Map (WSM) project is given, and the global database for contemporary tectonic stress orientation data of the Earth's crust is presented. This includes the statistics of stress data related to the stress determination method used, and the distribution of stress records versus depth. The quality ranking of WSM data most

appropriate to rock mechanics and rock engineering purpose is presented and discussed.

## 2.1 Historical Aspects

In the WSM project, a global database for contemporary tectonic stress data of the Earth's crust is compiled. It was originally compiled by a research group as part of the International Lithosphere Programme (Zoback et al. 1989). During the time period 1995–2008, the WSM Project was a research project of the Heidelberg Academy of Science and Humanities, Germany located at the Institute of Geophysics at Karlsruhe University, Germany (Heidbach et al. 2008). Since 2009, the home of the World Stress Map Project is the German Research Centre for Geosciences (GFZ) at Potsdam, Germany (Heidbach et al. 2010).

The first release of the WSM database contained 3,574 data records (Zoback et al. 1989) and the second one approximately 7,300 data records (Zoback 1992). The major findings of the first phase of the WSM project are published in a special Volume of the

Journal of Geophysical Research edited by Mary Lou Zoback (JGR Vol. 97). In this first phase of WSM, the compilation of data was primarily hypothesis-driven to investigate the plate boundary forces (including mantle drag) and to answer the question to what extent these forces are causing the long wave-length stress patterns. The focus of WSM was on stress data reflecting the large-scale contemporary tectonic intra-plate or midplate stress field (i.e., plate scale stresses) rather than details and complexities close to plate boundaries where the overall kinematics and deformation is quite well known (Müller et al. 1992; Zoback 1992). In the second phase of the WSM project between 1996 and 2008, this philosophy has changed to a data-driven compilation. In this period, there was an almost three-fold increase of stress data records; the current WSM database contains 21,750 data records, see Fig. 1. A few of the major conclusions derived from the analysis of the information in the WSM are that (1) over broad regions in the interior of many plates of the Earth's lithosphere are characterized by uniformly and consistently oriented horizontal stress

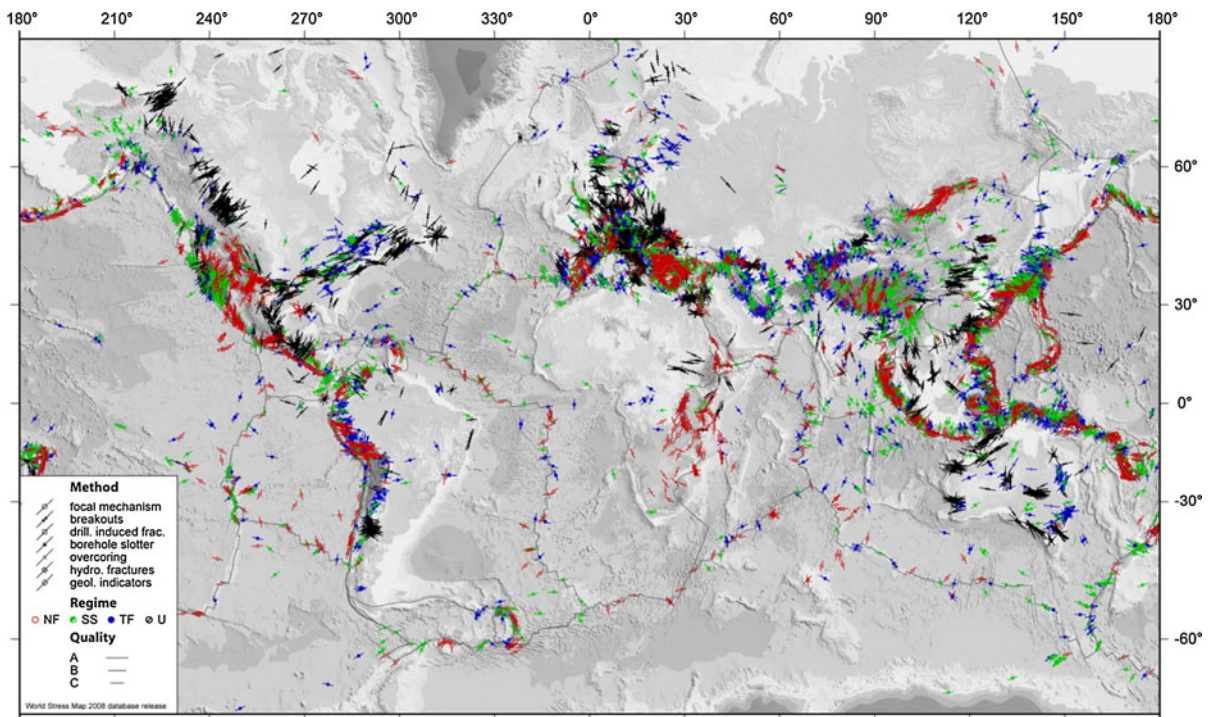


**Fig. 1** World Stress Map based on A–C quality data records of the WSM database release 2008, excluding all Possible plate Boundary Events (PBE) (Heidbach et al. 2010). Bars with symbol indicate  $S_H$  orientations according to stress determination technique, and bar length is proportional to data quality.

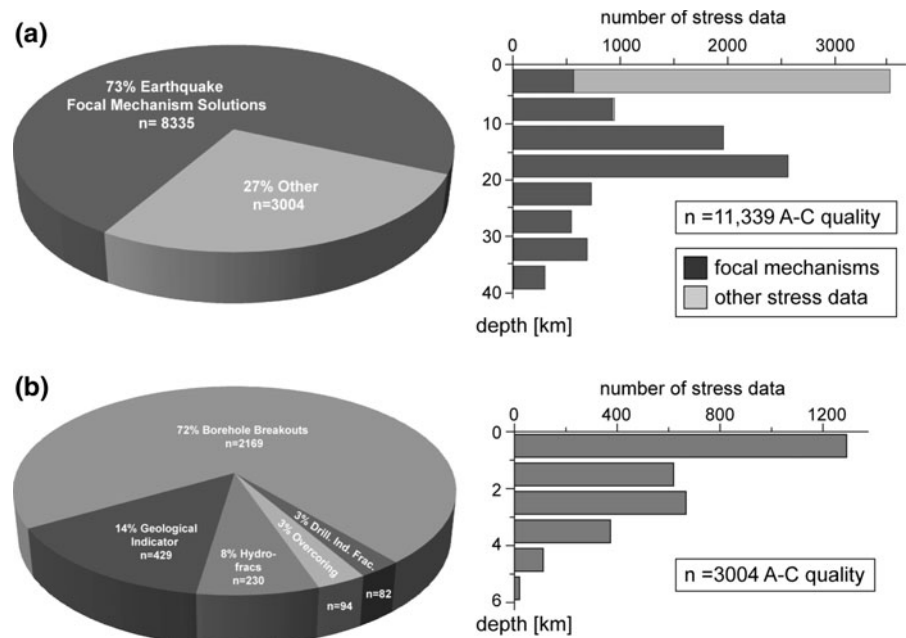
Colours indicate stress regimes with red for normal faulting (NF), green for strike-slip faulting (SS), blue for thrust faulting (TF), and black for unknown regime (U). Plate boundaries are taken from the global model PB2002 of Bird (2003)

fields like eastern North America, western Europe, the Andes, the Aegean; (2) most mid-plate or intra-plate continental regions are dominated by compressive stress regimes in which one or both horizontal stresses are greater than the vertical stress; and (3) in continental extensional stress regimes where normal or strike-slip stress field exist the maximum principal stress is vertical and generally occur in topographically high area. In the compilation shown in Fig. 1, all stress information of sufficient quality is added to the database regardless if the individual stress data point is representative for a larger region or not. In particular, the sedimentary basin initiative leads to a major increase of stress data records in areas that very much likely do not represent the long-wave length pattern, but local stress heterogeneities instead (Roth and Fleckenstein 2001; Tingay et al. 2005a, b, 2009; Heidbach et al. 2007). This evolution of WSM database into more local and shallow details of the in situ stress makes the project more attractive for geoengineering and geotechnical applications (Fuchs and Müller 2001; Tingay et al. 2005b; Henk 2008).

Various academic and industrial institutions working in different disciplines of Earth sciences such as geodynamics, hydrocarbon exploitations and rock engineering use the World Stress Map. The uniformity and quality of the WSM data is guaranteed through (1) quality ranking of the data according to an

internationally accepted scheme, (2) standardized regime assignment and (3) analysis guidelines for various stress indicator. To determine the  $S_H$  orientation, different types of stress indicators are used in the WSM database. The 21,750 data records of the latest database release 2008 are grouped into four major categories with the following percentage values (Heidbach et al. 2010): (1) earthquake focal mechanisms (72 %), (2) wellbore breakouts and drilling induced fractures (20 %), (3) in situ stress measurements like overcoring, hydraulic fracturing and borehole slotter (4 %), and (4) young geologic data from fault slip analysis and volcanic vent alignments (4 %). In Fig. 2, A–C quality data are separated into the percentage values of each individual method used for stress estimation. In Fig. 2a, the dominating portion of the pie chart are stress data from earthquakes (73 %), which show a depth distribution down to 40 km. In Fig. 2b, the focus is on borehole related stress data and geological stress indicator valid for shallow depth above 6 km (27 % of the pie chart from Fig. 2a). Individual stress indicators reflect the stress field of different rock volumes (Ljunggren et al. 2003), and different depths ranging from surface to 40 km depth (Heidbach et al. 2007). Fault plane solutions related to large earthquakes (Angelier 2002) provide the majority of data. Below 6 km depth, earthquakes are the only stress indicators available, except from a few ultra-

**Fig. 2** Statistics of  $S_H$  orientation data with A–C quality ( $n = 11,339$ ) data records. **a** With and **b** without earthquake related stress records ( $n = 3004$ ). *Left* pie charts, *right* depth sections





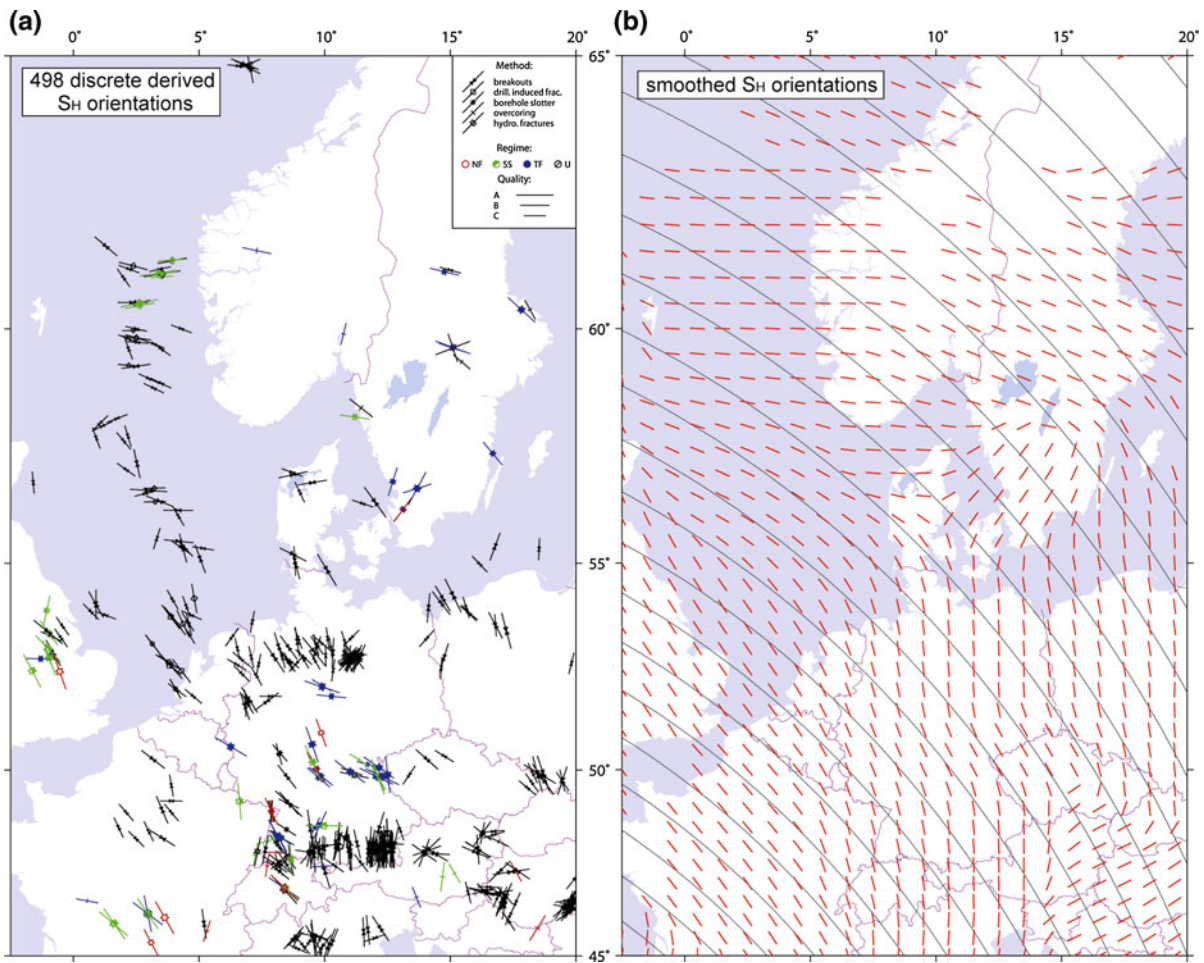


**Fig. 3** Stress maps of central and northern Europe. **a** Bars with symbols indicate the orientation of maximum horizontal stress  $S_H$  with bar length proportional to data quality. Only A–C quality data records from overcoring, borehole breakouts, drilling induced fractures and hydraulic fracturing of the WSM database release 2008 are shown. **b** Red bars indicate

smoothed  $S_H$  orientations on a regular grid using the smoothing algorithm of Müller et al. (2003). Thin black lines display the trajectories of relative plate movement of Africa with respect to Eurasia after DeMets et al. (2010). The search radius for the mean  $S_H$  orientation at each grid point is 250 km and the minimum number of data records within a search radius is  $n = 5$

deep drilling projects (Fig. 2b). In general, the relatively small percentage of in situ stress measurements is due to the demanding quality of the ranking scheme and the fact that many of the data are company owned.

### 2.2 Quality Ranking of WSM Stress Data for Rock Mechanics and Rock Engineering

The success of the WSM stress data compilation is based on a standardized quality ranking scheme for the individual stress indicators making them comparable on a global scale. The quality ranking scheme was introduced by Zoback and Zoback (1989) and Zoback

and Zoback (1991), and refined and extended in the work by Sperner et al. (2003) and Heidbach et al. (2010). Details on the quality ranking scheme can be found on the WSM website (<http://www.world-stress-map.org>). The scheme is internationally accepted and guarantees reliability and global comparability of the stress data. Each stress data record is assigned a quality between A and E, with A being the highest quality. A—quality means that the orientation of  $S_H$  is accurate to within  $\pm 15^\circ$ , B—quality to within  $\pm 20^\circ$  and C—quality to within  $\pm 25^\circ$ . In general, A–C quality stress data are considered reliable for the use in analyzing stress patterns (cf. Figs. 1, 2, 3).

**Table 1** World Stress Map (WSM) quality ranking system for rock mechanics and rock engineering

Stress indicator	Quality A $SH \pm 15^\circ$	Quality B $SH \pm 15\text{--}20^\circ$	Quality C $SH \pm 20\text{--}25^\circ$
Borehole breakouts (BBO)			
From caliper logs	$\geq 10$ distinct breakout and combined length $\geq 300$ m in a single well with s.d. $\leq 12^\circ$	$\geq 6$ distinct breakout and combined length $> 100$ m in a single well with s.d. $\leq 20^\circ$	$\geq 4$ distinct breakouts and combined length $\geq 30$ m with s.d. $\leq 25^\circ$
From image logs	$\geq 10$ distinct breakout zones and combined length $\geq 100$ m in a single well with s.d. $\leq 12^\circ$	$\geq 6$ distinct breakout zones and combined length $> 40$ m in a single well with s.d. $\leq 20^\circ$	$\geq 4$ distinct breakouts and combined length $\geq 20$ m with s.d. $\leq 25^\circ$
Drilling induced fractures (DIF)	$\geq 10$ distinct fracture zones in a single well with a combined length $\geq 100$ m and s.d. $\leq 12^\circ$	$\geq 6$ distinct fracture zones in a single well with a combined length $\geq 40$ m and s.d. $\leq 20^\circ$	$\geq 4$ distinct fracture zones in a single well with a combined length $\geq 20$ m and s.d. $\leq 25^\circ$
Hydraulic fracture (HF)	$\geq 5$ hydrofrac orientations in a single well with s.d. $\leq 12^\circ$ depth $\geq 300$ m, and distributed over a depth range $\geq 300$ m	$\geq 4$ hydrofrac orientations in a single well with s.d. $\leq 20^\circ$ depth $\geq 100$ m, and distributed over a depth range $\geq 200$ m	$\geq 3$ hydrofrac orientations in a single well with s.d. $\leq 25^\circ$ depth $\geq 30$ m, and distributed over a depth range $\geq 100$ m
Overcoring (OC) and borehole slotter (BS)	$\geq 11$ measurements with depth $\geq 300$ m and s.d. $\leq 12^\circ$	$\geq 8$ measurements with depth $\geq 100$ m and s.d. $\leq 20^\circ$	$\geq 5$ measurements with depth $\geq 30$ m and s.d. $\leq 25^\circ$

In Table 1, we show a subsection of the WSM quality ranking system with relevance to most rock mechanics and rock engineering applications. For this purpose, only borehole-scale stress indicators of A–C quality are listed. This includes the quality ranking of borehole breakouts, separated into different ranking schemes for breakouts interpreted with four-arm calipers and breakouts interpreted on image logs. The quality ranking of drilling induced fractures has been refined to better reflect the ability for different log types to reliably determine the contemporary stress orientation. It has to be emphasized that for practical stress estimates in rock mechanics and rock engineering sized volumes, we recommend to rely on the three most important methods like overcoring (Ljunggren et al. 2003), hydraulic techniques (Haimson 1978; Haimson and Cornet 2003; Sano et al. 2005) and borehole breakout analysis (Bell and Gough 1979; Bell 1990; Haimson and Lee 1995; Haimson 2007).

### 3 Stress Orientation Maps

At the very first stage of estimating the state of stress at a site or a region, consultation of the WSM database is appropriate and often worthwhile. A detail map of the area of interest can be generated with the online tool

CASMO (Create A Stress Map Online) on the website of the WSM project. The generated stress map contains a legend of the most likely type of stress regime (normal, strike-slip and thrust faulting regime) in the area. Data can also be extracted from different depth intervals and for different stress recording methods (cf. Fig. 2). Provided sufficient stress data are available a smoothed stress map can be generated. As an example, Fig. 3 shows a map with the smoothed  $S_H$  orientation on a regular grid of Central and Northern Europe. The map displays both, the original 498 WSM data records from borehole breakouts, hydraulic fracturing, drilling induced fractures and overcoring with A–C quality limited to depth shallower than 6 km (Fig. 3a, short bars with symbols) and the smoothed stress field based on a regular spaced grid in the background (Fig. 3b). Data records of the WSM database release 2008 are shown, neglecting data from earthquake focal mechanism solutions (FMS) and stress inversion of focal mechanism solutions (FMF). This is, because for stress estimates in rock mechanics and rock engineering sized volumes, the use of in situ stress data from overcoring, breakouts and hydraulic methods are most suitable. In Fig. 3b, red bars indicate smoothed  $S_H$  orientations on a regular grid using the smoothing algorithm described in detail in Müller et al. (2003) with a search radius,  $R$  of 250 km ( $R = 250$  km) and a

minimum number,  $n$  of three data records within the search radius ( $n = 3$ ). Curved, thin black lines display the trajectories of relative movement of the Africa plate with respect to the Eurasian plate using the Eulerian pole described in DeMets et al. (1994, 2010). In general, the first-order approximation of the stress pattern in Fig. 3 shows a prevailing NW to NNW  $S_H$  orientation, which is mainly explained by plate boundary forces, in particular by ridge push of the North Atlantic and the collision of the Africa Plate with the Eurasia Plate (Müller et al. 1992). However, from West to East one can clearly see the fan-shaped pattern of the  $S_H$  orientations. This is explained with the large density contrast of the crustal thickness increase from Western Europe to the European craton (Grünthal and Stromeier 1994; Heidbach et al. 2007). In Fig. 3b, note that the deviation between the smoothed stress pattern and the relative plate motion is much larger compared to the previous publication (Heidbach et al. 2007) where also the data from earthquake focal mechanisms are used. This confirms that in the upper part of the crust (shallow depths above 6 km), the variability of  $S_H$  orientation based on borehole stress data is significantly higher.

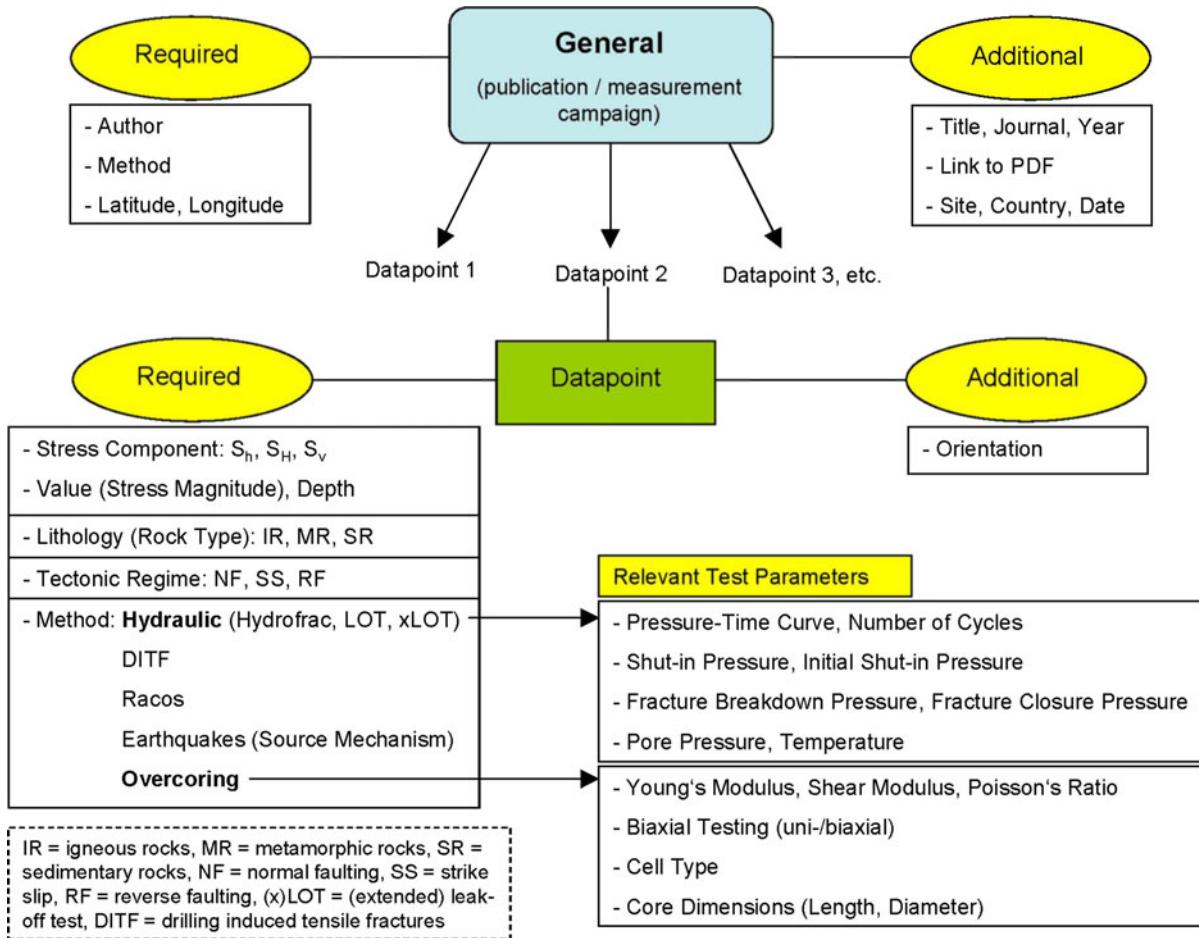
#### 4 Lithologic Stress Magnitudes

Many authors have collected and summarized data on rock stresses and proposed expressions for the variation of the magnitude of the vertical and horizontal stresses with depth at specific sites and/or regions of the world. A summary of references to publications of horizontal and vertical stresses versus depth, magnitude-depth profiles and stress orientation maps are presented in Amadei et al. (1987) and Zang and Stephansson (2010), respectively. When estimating the state of stress at any depth in the rock mass, we make the assumption that the state of stress can be described by three principal stress components: a vertical component due to the weight of the overburden at that depth and two horizontal components which are larger or smaller than the vertical stress. For the variation of vertical stress with depth, there has been a long series of in situ stress measurements conducted and several data compilations done (Herget 1974; Brown and Hoek 1978; Amadei and Stephansson 1997), that proves that, in most cases, the magnitude of the vertical stress can be explained by

the overburden weight only. Deviation from this rule exists and in particular in areas of young tectonics, volcanism, rough topography near major discontinuities in the rock mass. Relationship between vertical and horizontal stress for simple, elastic, homogeneous Earth, and rock masses with transversely and orthotropic anisotropy are presented in Tonon and Amadei (2003) and Zang and Stephansson (2010). The authors (Heidbach et al. 2010; Zang and Stephansson 2010) have pointed out that the generic, often linearly increasing stress magnitude versus depth relationships presented, should be used with caution, as they are usually associated with scatter. The stresses at a site can vary locally due to topography, geological unconformities, stratification, geological structures such as faults, dikes, veins, joints, folds etc. Therefore, in estimating the state of stress at a site or a region these local perturbations need to be considered (Lund and Zoback 1999; Lin et al. 2010; Rasouli et al. 2011) as they cause deviation from the often-assumed linearity of stress changes with depth.

#### 4.1 Further Developments of WSM

Currently the WSM database is developed further. Besides the standard procedure to add further data records of  $S_H$  orientations, we recently started to compile data on stress magnitudes in a second database. We believe this development will be of interest and use for the rock engineering community. A prototype input template has been designed to incorporate information on stress magnitudes into the new Q-WSM database (Table 2). Each data entry gives information on one or more of the in situ stress magnitudes (i.e., vertical  $S_V$ , maximum horizontal  $S_H$ , minimum horizontal  $S_h$ ) for a certain depth range. Among the methods used to determine stress magnitudes are hydraulic fracturing, leak-off tests, overcoring, undercoring, core-based methods and source mechanisms of earthquakes (relative stress ratios). For each method, the input template keeps ready specific parameters relevant for the technique involved (Table 2, relevant test parameters) which need to be known in order to judge the stress magnitudes. We follow the subdivision of stress magnitude measurements from Zoback (2007),  $S_V$  to be determined from cuttings or density logs,  $S_h$  from hydraulic fracturing (Hubbert and Willis 1957), leak-off tests (LOT, e.g., Bell 1990) and extended leak-off

**Table 2** Metadata and prototype input template in Quantitative World Stress Map (Q-WSM)

tests (xLOT, e.g., Lin et al. 2008), and constraints for  $S_H$  from drilling-induced tensile failure (e.g., Li and Schmitt 1998) and borehole breakout analysis taking into account the width and depth of breakouts (e.g., Barton et al. 1988, Shen 2008). For determining stress magnitudes from drill cores, we follow the subdivision of methods and terminology developed by Zang and Stephansson (2010). Information on relative stress magnitudes from earthquakes are deduced from fault plane solutions and formal stress tensor inversion (cf. WSM homepage). We intend to come up with a quality ranking system for the stress magnitudes in analogy to the ranking system for the stress orientations (cf. Table 1). The rock type (lithology) and tectonic stress regime are additional pieces of information in the corresponding stress magnitude input template (Table 2, data record required), which will

become available online. Together with the  $S_H$  orientation in WSM database, the stress magnitudes in the new Q-WSM database become a more quantitative tool to describe stresses in the Earth's crust. Particular for rock mechanics and rock engineering applications, the Q-WSM will become an indispensable source of information to collect prior to any new stress measurements planned at a site, area or region.

As an example of an exemplary data entry into the Q-WSM database of stress magnitudes, we refer to the core-based prediction of lithologic stress contrasts in East Texas formations (Thiercelin and Plumb 1994). In here, the downhole stress state is characterized by minimum stress magnitude, vertical stress, pore pressure, effective stresses and effective stress coefficients. Rock properties listed include the Young's modulus and Poisson's ratio, and also account for rock



anisotropy in sandstones, mudstones and shales. Rock strength properties are based on uniaxial tests and triaxial fracture and frictional strength tests. In this way, the Thiercelin and Plumb (1994) data compilation in the depth range 1,879–2,912 m serves an ideal set of data entries into Q-WSM. For other entries, however, the information on rock testing in the laboratory (drained, undrained) is sometimes limited, or in the worst case missing. This will affect the quality of the Q-WSM data point.

#### 4.2 Quantitative World Stress Map, Q-WSM

In the following, we discuss first results of the new Q-WSM database containing 1,278 data records of single stress magnitudes taken from published literature. Stress magnitudes in Q-WSM are absolute stresses, not effective stresses. If more pore pressure data sets become available, there will be an option in Q-WSM to choose either absolute or effective stress magnitudes for different plot types. Figure 4 indicates the methods used for determining the stress magnitudes (Fig. 4a), and the location the stress data come from world-wide (Fig. 4b) and within Europe (Fig. 4c). Most stress magnitudes are obtained through hydraulic fracturing (Fig. 4a, 77 %) where  $S_h$  is the most reliable value determined from the shut-in pressure of the fractured rock formation (Amadei and Stephansson 1997; Haimson and Cornet 2003). Overcoring stress magnitudes account for 16 %. Most of the data records collected so far come from Asia, Europe and North-America (Fig. 4b). Within European countries apart from Iceland, the dominating portion of stress magnitudes comes from France (Cornet and Burlet 1992), UK and Switzerland

(Fig. 4c). The reason for this may be the many tunnelling projects and site characterization of radioactive waste disposal sites where stress magnitudes and orientation are of utmost importance in planning and designing the underground excavation (Wileveau et al. 2007). The experience of stress measurements related to site characterization for radioactive waste disposal is the relatively long time and many measurements needed to have a proper understanding of the stress field including its magnitudes versus depth for an area of about a square kilometre or so.

There are a number of ways of displaying profiles of stress magnitudes versus depth in the Earth’s crust (Zang and Stephansson 2010). One way is to plot the two horizontal and vertical stress components with depth, or the mean horizontal stress. McGarr (1980) used maximum shear-stress data, Stephansson et al. (1986) preferred mean-stress data, and Engelder (1993) octahedral shear stress versus depth. A second way, is to use dimensionless stress ratios rather than stress magnitudes. Among them, the lateral-stress coefficient (Van Heerden 1976; Brown and Hoek 1978), the ratio of maximum horizontal to vertical stress (Bieniawski 1984) and the ratio of minimum horizontal to vertical stress (Rummel et al. 1986; Herget 1987; Savage et al. 1992) have been used. In addition, Sen and Sadagah (2002) introduced a probabilistic approach for the lateral stress coefficient variations at any given depth.

In this contribution, we follow the pragmatic way suggested by Brown and Hoek (1978) interpreting collected worldwide stress data in terms of the vertical stress ( $S_V$ ) and the lateral-stress coefficient ( $k = 0.5(S_h + S_H)/S_V$ ) to demonstrate generic trends in our Q-WSM database, but here we distinguish in terms

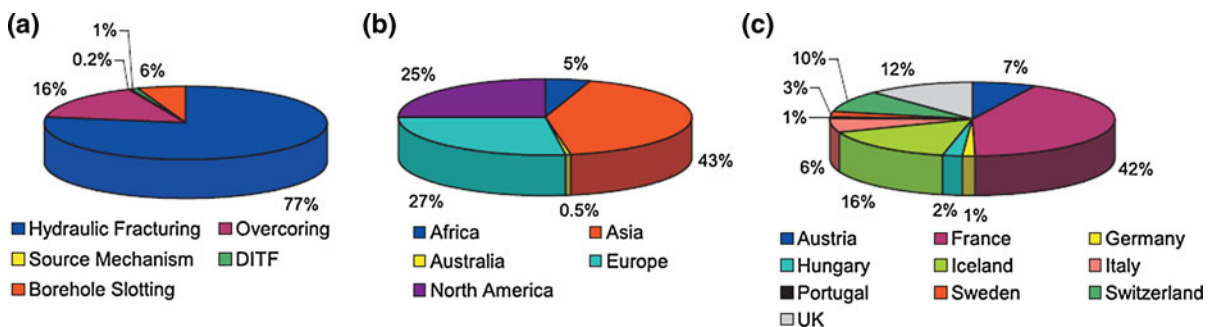
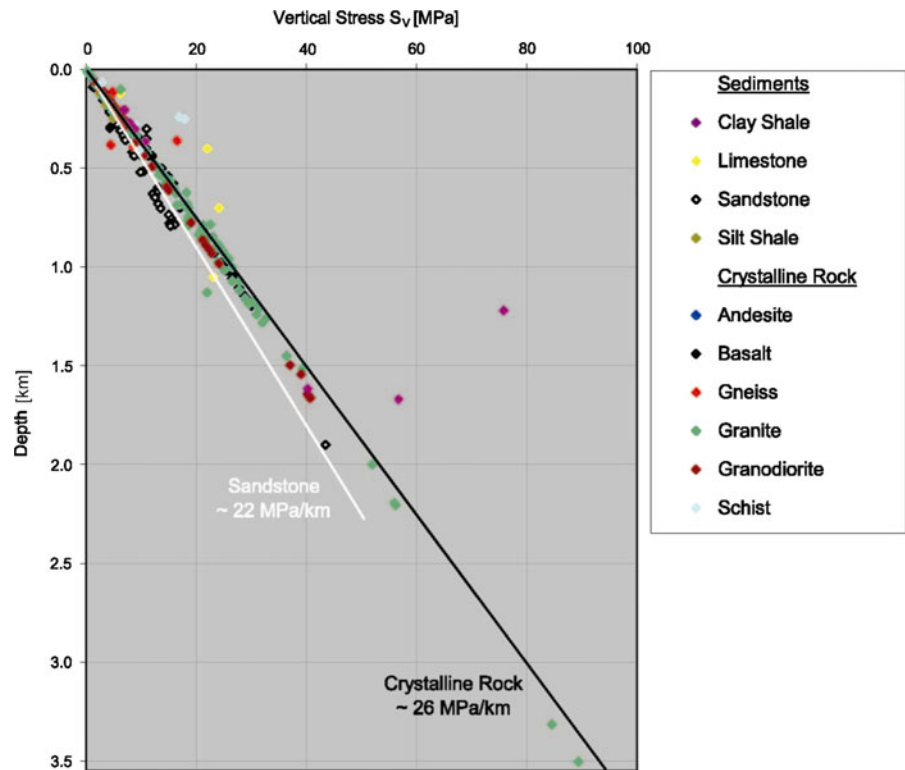


**Fig. 4** Statistics of in situ stress magnitude data ( $n = 1278$ ). Pie chart of **a** stress magnitude determination technique, **b** distribution of worldwide magnitudes, and **c** distribution of European stress magnitudes

**Fig. 5** Absolute lithologic stress magnitudes versus depth for the vertical stress component,  $S_V(z)$



of lithology. In Fig. 5, the vertical stress is plotted versus depth for different rock types. According to this limited database, crystalline rock account for an overburden pressure gradient of 26 MPa/km while sandstones are characterized by a vertical stress gradient of 22 MPa/km. For comparison, the average vertical stress gradient in Brown and Hoek (1978) corresponds to 27 MPa/km with no assignment to rock types. Different stress gradients may come from different regions analyzed, and rock types not taken into account. So far, in Q-WSM, 70 % of the stress magnitude data come from Asia and Europe (cf. Fig. 4) as compared to stress magnitude and stress ratio data ( $S_V$ ,  $k$ ) in Brown and Hoek (1978) mainly taken from Australia, Canada, USA and Southern Africa. The vertical stress component is correct in the sense of a linear best-fit regression line (cf. Fig. 5). Deviations are due to variations in local topography, geologic heterogeneities, and rock anisotropy. In some cases,  $S_V$  differs by about five times the predicted component. One example for determining anisotropic stress in anisotropic rock is given in Hakala et al. (2007), investigating mica gneiss from Olkiluoto, Finland. In this case, a correction of the local stress

magnitudes by quantifying anisotropic rock properties needs to be found in order to determine the in situ state of stress at the site reliably. Other studies taking into account the effect of rock anisotropy on stress, are Amadei et al. (1987) and Tonon and Amadei (2003). In general, however, generic unit weights of selected rock types (sandstones or crystalline rock, cf. Fig. 5) can provide a good predictive estimate of the averaged vertical stress versus depth. For borehole stress estimates, the variation of rock density with depth has to be measured, e.g., from drill cores or cuttings while a bore hole is penetrated into the Earth's crust (e.g., Zoback et al. 2003).

In Fig. 6, the dimensionless stress coefficient,  $k$  is plotted versus depth for crystalline (Fig. 6a) and sedimentary rock (Fig. 6b). At shallow depths, the  $k$ -value is found to increase to values up to  $k = 9.5$  for crystalline rock (at 100 m depth) and up to  $k = 7.5$  for sedimentary rock (at 300 m depth). At greater depth, the range of  $k$  narrows considerably, and at depth greater than 3 km the observed values are generally less than 1. Neither Heim's rule ( $k = 1$ ) nor the biaxial stress model ( $k = 1/3$ , assuming Poisson's ratio equal to  $1/4$ ) provide a good explanation for the data trends,

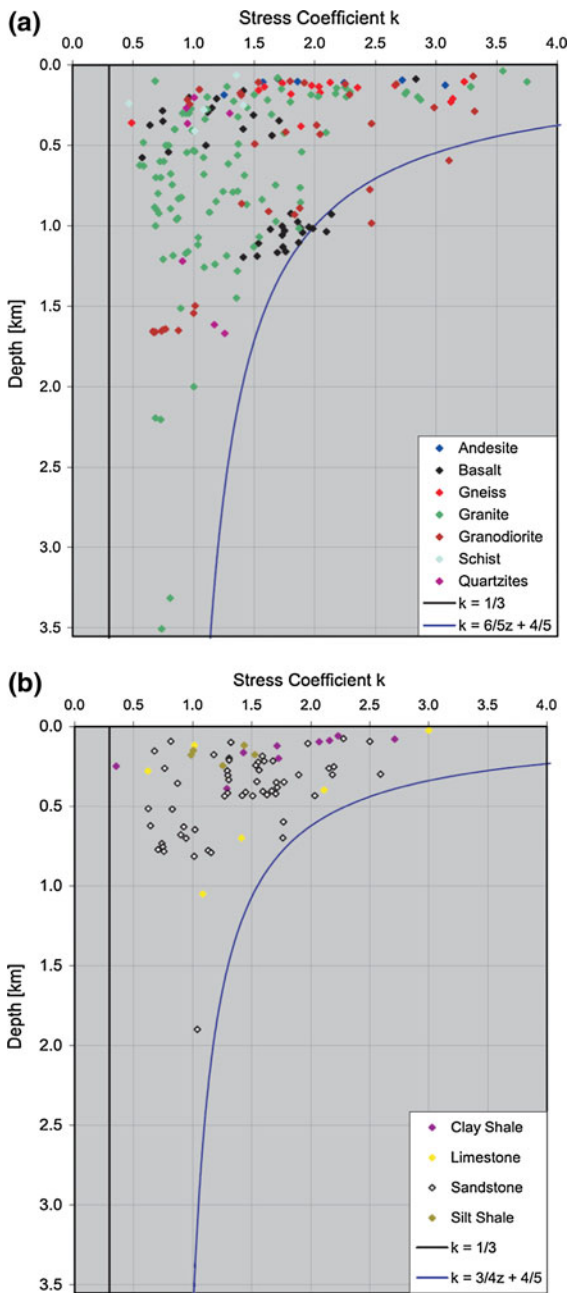


**Fig. 6** Absolute lithologic stress coefficients versus depth,  $k(z)$  for **a** crystalline, and **b** sedimentary rocks. Lower bound is based on the biaxial stress model ( $k = 1/3$ ), and the upper bounds result from the spherical shell model

which show a highly nonlinear decrease of  $k$  value with depth. Therefore, Brown and Hoek (1978) fitted two envelopes that provide rough bounds to the data ( $0.1/z + 0.3 \leq k \leq 1.5z + 0.5$ ), where  $z$  is taken in kilometres. Both curves are of the same algebraic

form,  $k = a/z + b$ , as is predicted by a spherical shell model of the Earth’s crust (e.g., McCutchen 1982; Sheorey 1994; Aydan 1995). In this model, the crust is taken to be a thin, elastically isotropic and homogeneous shell, resting on top of a thermo-elastic mantle and deforming due to gravity. Assuming the thickness of the crust to be very small compared to the Earth’s radius, the asymptotic values of 0.3 and 0.5 for the rough bounds correspond to the values predicted by a spherical shell model if the Poisson ratio,  $\nu$  of the rock is varied between 0.23 and 0.33. Data in Fig. 6 are limited to  $k \leq 4$ , and the upper boundary of the curve is adapted to the lithology used (Fig. 6a:  $k = 6/5z + 4/5$  for hard rock, Fig. 6b:  $k = 3/4z + 4/5$  for sedimentary rocks). For the lower bound, we used the stress coefficient of the biaxial stress model (Fig. 6:  $k = \nu(1 - \nu)^{-1} = 1/3$ ). Most stress coefficients fall within these bounds, except for five crystalline data records between  $\sim 0.6$  and  $\sim 1.1$  km (three granodiorites and two basalts). The convergence of  $k$ -values to a value of unity at depth greater than 3 km is consistent with the principle of time-dependent elimination of shear stress in rock (Heim’s rule,  $k = 1$ ). The final conclusion from inspection of Fig. 6, however, is that in situ stress bounds for  $k$ -values in rock from the simple spherical shell model seem to have different bounds for different rock types. This needs to be proven in future with a more dense Q-WSM stress magnitude data set.

In Fig. 7, we plotted the stress magnitudes in 2D stress space. Figure 7a shows the minimum and maximum horizontal stress for all data entries. Data cluster around the linear regression line  $S_h = 0.57S_H$ . This can be an artefact of too few stress magnitudes used ( $n = 1,278$ ), or this can demonstrate the fact that  $S_H$  is mostly derived from direct correlation with  $S_h$ . This direct correlation includes assumptions about the friction coefficient in rock which are commonly used to calculate  $S_H$  from measured  $S_h$  values with independent knowledge of rock strength, the vertical stress and in case of effective stresses, the pore pressure of the formation (Bell 1990; Zoback et al. 2003). Note that the  $S_H$  magnitude in Fig. 7 is the most difficult component of the stress tensor to accurately estimate, and therefore the component of the stress tensor with the largest error bar. This will be discussed in chapter 5 in more detail. In Fig. 7b, the two horizontal stress components are plotted versus the vertical stress magnitude for all data entries.

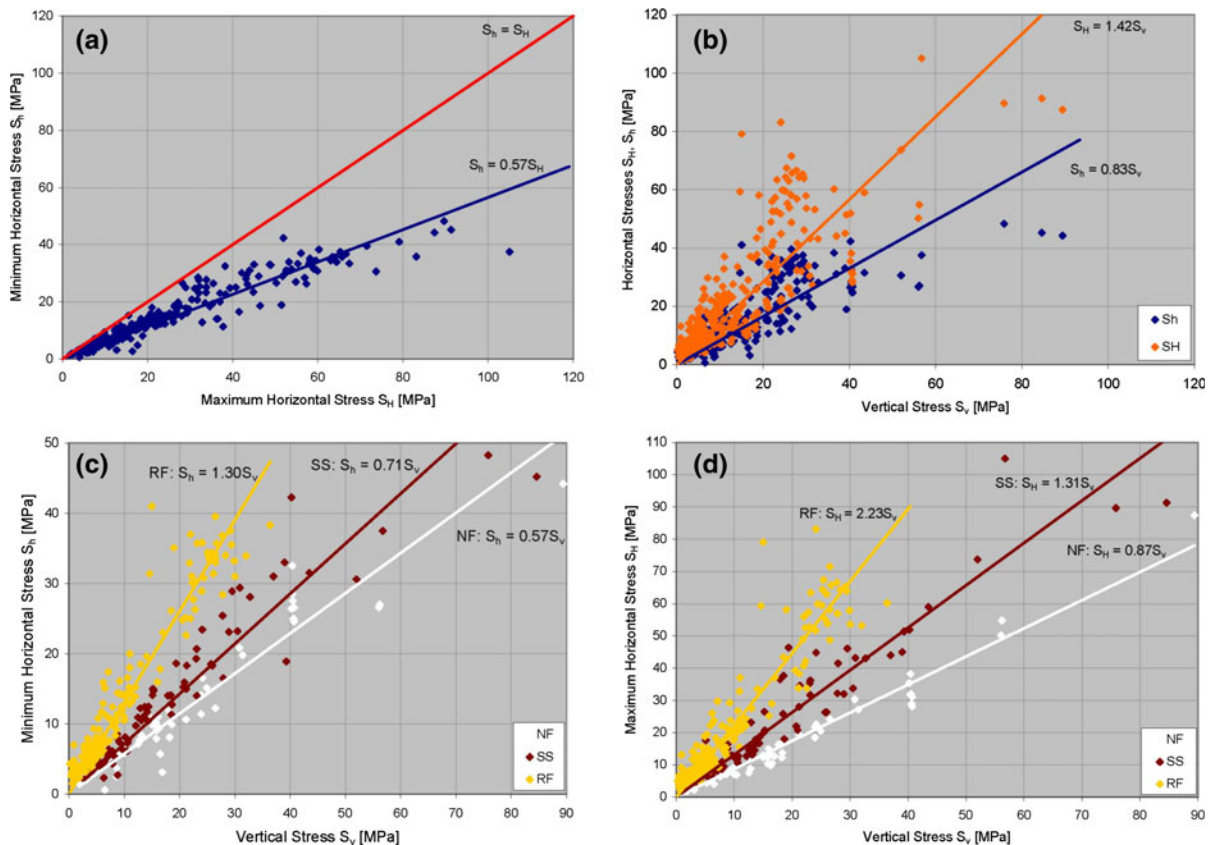


**Fig. 7** Absolute stress magnitudes in 2D stress space, influence of tectonic faulting regime. **a** Minimum horizontal versus maximum horizontal stress component,  $S_h(S_H)$ , and **b**, the two horizontal stresses versus the vertical stress component,  $S_{h,H}(S_v)$ . **c** Minimum horizontal versus vertical stress

component,  $S_h(S_v)$ , and **d** maximum horizontal versus vertical stress component,  $S_H(S_v)$ . In (c) and (d), data sets are separated according to tectonic faulting regimes (NF normal, SS strike-slip, RF reverse faulting)

Independent of faulting regime, the Q-WSM data sets show a slope of  $S_h/S_v = 0.83$  and  $S_H/S_v = 1.42$ . The scatter, however, is more pronounced as compared to the horizontal stress ratio (cf. Fig. 7a,  $S_h = 0.57S_H$ ). In Fig. 7c, the minimum horizontal stress, and in Fig. 7d, the maximum horizontal stress are plotted versus the vertical stress, but in contrast to the previous figures separated according to tectonic faulting regime. From this it follows, that the ratio  $S_h/S_v$  varies from 0.57, 0.71 to 1.30 using normal faulting (NF), strike-slip faulting (SS), and reverse faulting (RF) as discriminator, respectively (Fig. 7c). The largest difference in stress ratios, however, is observed when the maximum horizontal and vertical stress component is involved, i.e.,  $S_H/S_v = 0.87, 1.31, 2.23$  for NF, SS and RF, respectively (Fig. 7d). Stress ratios discussed in Fig. 7, are in agreement with limits on in

situ stress from frictional strength of faults (Scholz 2002; Zoback 2007). Assuming a friction coefficient  $\mu = 0.6$ , in a normal faulting regime the lower bound of the minimum horizontal stress is  $S_h \sim 0.6S_v$ . The value of  $S_h$  cannot be lower than this value because well-oriented NF would slip. In reverse faulting regimes, the limiting value is  $S_H \sim 2.2S_v$  for hydrostatic pore pressure and  $\mu = 0.6$ .

In Fig. 8, we plotted Q-WSM stress magnitudes in 2D stress space but separated data entries according to lithology. As expected, the relationship between minimum and maximum horizontal stress is almost not affected by rock type. The ratio is found to be  $S_h/S_H = 0.56$  for crystalline rock (Fig. 8a),  $S_h/S_H = 0.61$  for sedimentary rock (Fig. 8b), and does not change significantly when compared to the value for all rock types (Fig. 7a,  $S_h/S_H = 0.57$ ). This confirms that the



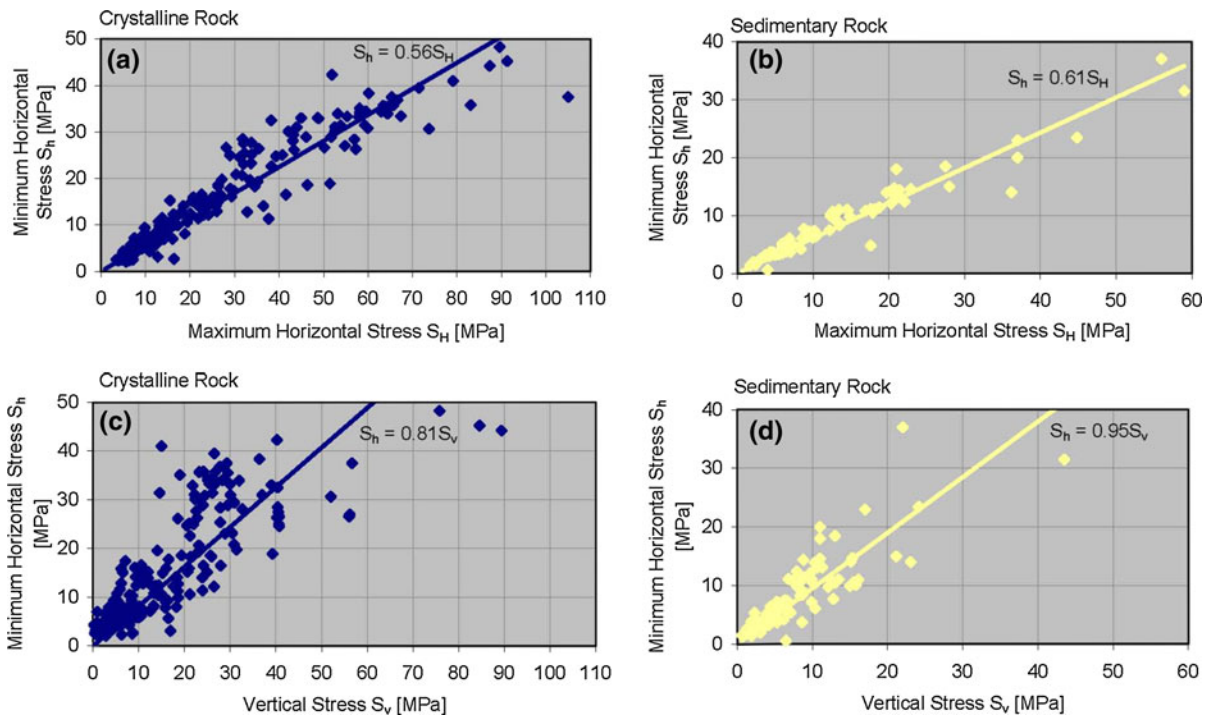


**Fig. 8** Absolute stress magnitudes in 2D stress space, influence of lithology. Minimum horizontal stress versus maximum horizontal stress component,  $S_h(S_H)$  for **a** crystalline, and

**b** sedimentary rock. Minimum horizontal stresses versus vertical stress component,  $S_h(S_v)$  for **c** crystalline, and **d** sedimentary rock

**Table 3** Lithologic and tectonic stress ratios from Q-WSM database

Stress ratio	Rock type		Tectonic faulting regime			Total
	Crystalline, 221	Sedimentary, 75	NF, 49	SS, 74	RF, 173	
$N$						$N = 296$
$S_h/S_H$	0.56	0.61	0.64	0.53	0.57	0.57
$(R^2)$	(0.91)	(0.93)	(0.86)	(0.84)	(0.97)	(0.91)
$S_h/S_v$	0.81	0.95	0.57	0.71	1.30	0.83
$(R^2)$	(0.67)	(0.69)	(0.91)	(0.89)	(0.92)	(0.69)
$S_H/S_v$	1.41	1.54	0.87	1.31	2.23	1.42
$(R^2)$	(0.64)	(0.71)	(0.97)	(0.90)	(0.87)	(0.66)

$N$  number of data records,  $R^2$  coefficient of linear regression,  $NF$  normal faulting,  $SS$  strike-slip faulting,  $RF$  reverse faulting

estimation of  $S_H$  in published literature is mostly derived from direct correlation with  $S_h$  (determined from measurements in the field) and does not depend on lithology. The situation, however, is different when comparing rock-specific ratios of minimum and vertical stress components. The ratio turns out to be  $S_h/S_v = 0.81$  for crystalline rock (Fig. 8c) and  $S_h/S_v = 0.95$  for sedimentary rock (Fig. 8d). The scatter of data seems to be less going from the ratio with the

vertical stress involved to the ratio with the two horizontal stresses to be involved (direct dependence of  $S_H$  from  $S_h$ ). The scatter of data seems to be also less going from crystalline to sedimentary rocks (less data entries for sedimentary than for crystalline rock). For convenience, in Table 3 the summary of all possible combinations of stress ratios is displayed systematically, according to lithology and tectonic faulting regime based on data records with three stress

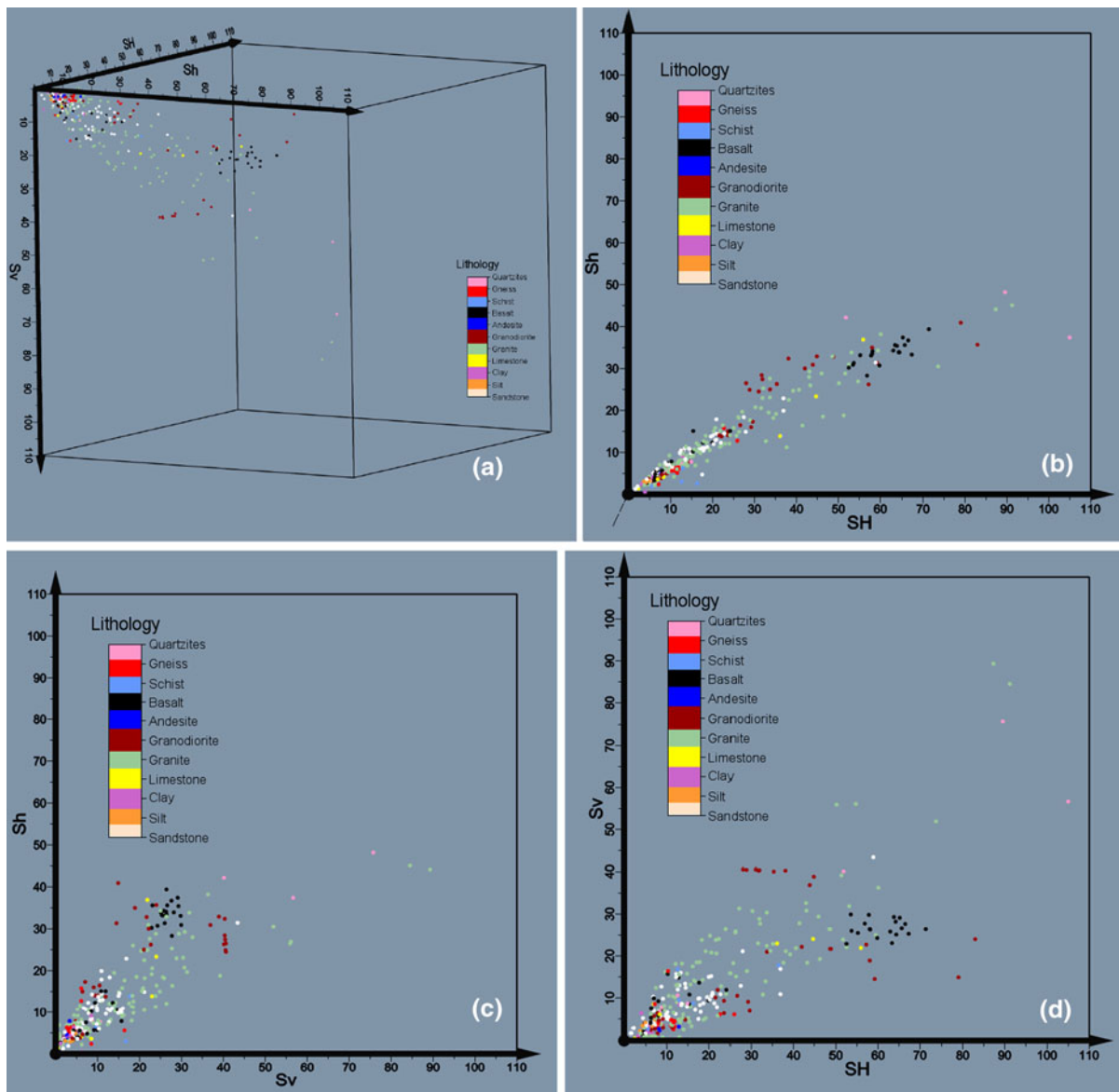


**Fig. 9** Absolute stress magnitudes for different rock types **(a)** in 3D stress space ( $S_h$ ,  $S_H$ ,  $S_V$ ), **b** in 2D cross section  $S_H$ – $S_h$ -plane, **c**  $S_h$ – $S_V$ -plane, and **d**  $S_H$ – $S_V$ -plane

magnitudes. In future statistics, ratios may change when more rock type-specific data will become available in Q-WSM.

In Fig. 9a, rock type-specific stress magnitudes from Q-WSM are plotted in 3D stress space as commonly used for visualizing rock failure criteria, e.g., from true-triaxial testing. For this purpose, a stress cube is shown spanned out by the two horizontal stress magnitudes ( $x$ - and  $y$ -direction), and the vertical stress magnitude ( $z$ -direction positive downwards).

The size of the cube is fixed by the upper limit of stress magnitudes for each stress component, i.e., 110 MPa in each direction. For  $S_V$ , this corresponds to  $\sim 4$  km depth. Colours indicate different rock types, whereby colours at the bottom of the lithology column refer to sedimentary rocks. This type of plot is designed to include rock strength parameters (uniaxial-, triaxial-, true-triaxial compressive strength) in future to address the question, how close the rock mass is to failure at depth. Displaying both, the state of in situ stress at

depth and the failure surface of corresponding rock can also be of important in slip tendency analyses when taking into account the orientation of the most critical fault plane. The rock is assumed to be intact at stress states inside the failure surface (Fig. 9a, all *dots* shown), while the rock mass fails for any stress state at the failure surface (Fig. 9a, not shown). Stress magnitudes measured and failure surfaces outlined in 3D need to be analyzed specifically for each rock type. Also the projections of data onto the cube's surfaces are shown (Fig. 9b–c).

## 5 Discussion

In this chapter, we first briefly discuss the use of stress orientation maps, in particular when the smoothing algorithm is applied. Second, we focus on the lateral stress coefficient, i.e., the stress ratios, which are discussed as a function of depth, rock types and faulting regimes. Finally, we comment on the investigation and reliability of stress magnitudes versus depth and in stress space.

### 5.1 Stress Orientation, WSM

Originally, the WSM project only accounts for  $S_H$  azimuth values for different depth, determined by different methods. The relationship between principal stresses is assigned in the faulting regimes (Fig. 1, colour coded bars). Ultimate depth for borehole related stress data is 6 km with very few exceptions from ultra-deep wells, and ultimate depth from earthquake related stress records is 40 km (Fig. 2). One smart tool for stress orientation analysis is the computation of smoothed  $S_H$  orientation maps (Fig. 3). For identifying stress patterns, i.e., coherent domains in which the orientation of  $S_H$  is constant, Fig. 3a is not very suitable because (1) there are large lateral fluctuations in data densities throughout Europe, (2) there is a wide spread in orientations at single locations where data density is high (clusters), and (3) there are error bars in any single location due to the data-quality ranking system within the World Stress Map. Because it is impossible for the human eye to take into account (1) to (3) at proper weight, the smoothing of stress orientation maps is required to identify trends (Fig. 3b). Smoothing stress orientations is a statistical method to estimate stress pattern

and stress trajectories based on observed stress orientation data. Smoothers aid in data analysis by revealing and enhancing pattern present in a set of measurements. This is accomplished by removing local fluctuation in data, while preserving large-scale trends. A review on the framework for the development of smoothers is given in Zang and Stephansson (2010).

The smoothing algorithm can be applied to the  $S_H$  orientation data in WSM with strong variation in lateral data density. To vary the region affected by the smoother explicitly allows resolving stress patterns at different scales. If the deviations between a smoothed  $S_H$  orientation and an observed one are too large, however, then probably no such stress pattern exists within the diameter of the search circle. Smoothed  $S_H$  orientation maps can be used as input for studies of plate tectonic problems, or at regional scale to set-up a geomechanical model. In this context, we have to calculate stress trajectory maps rather than gridded maps, as shown in Fig. 3b. Stress trajectory maps show a series of lines which are parallel and perpendicular to the directions of principal stresses. The number of trajectories needed to adequately describe a stress field depends on the smoothness of the field. A relatively large number of stress trajectories are required to characterise an irregular stress field (Isra and Galybin 2010). For detailed reservoir models, however, stress orientations smoothed or discrete are not sufficient to set up reasonable initial stress conditions for a geomechanical-numerical model that aims to quantify borehole failure, reactivation of sealing faults, and to predict optimal drilling pathways on fracture propagation. For these models knowledge of the absolute stress state and pore pressure are essential (see Sect. 1).

### 5.2 Stress Ratios, Q-WSM

Stress ratios and lateral stress coefficient versus depth allow to infer additional data as compared to WSM, which is essential at shallower depth ( $\sim 300$  to  $800$  m), i.e., for rock engineering purpose. When screening published literature for values of in situ stress magnitudes, we have to rely on the limited information of core testing procedures which are published together with the stress magnitudes. Sometimes, there is no information available whether the laboratory tests are carried out in drained or undrained conditions, or whether cores are drilled from intact

rock material or suffer from unloading and cooling cracks. In this way, we have to rate the Q-WSM magnitude entries in analogy to the WSM orientation entries by a quality ranking system. As indicated in Sect. 4.1, stress data from Thiercelin and Plumb (1994) can be regarded as ideal in situ stress magnitudes, and therefore will be rated A-quality. On the other hand, if information on pore pressure, and therefore effective stresses are missing, or elastic properties and fracture and friction strength of rock are not determined, the quality of the data entry will drop, and the error bar on stress magnitudes will become larger. For first insights into the Q-WSM stress magnitude database, however, we did not assign a quality ranking system, and cannot attach error bars to the stress magnitudes and stress ratios, except for the measurement errors indicated in the specific publication the data points come from. Nevertheless, we are able to discuss some generic trends.

In Fig. 6, we demonstrate with our limited database (1,278 records), the depth dependence of stress ratios in hard crystalline (Fig. 6a) and soft sedimentary rock (Fig. 6b). The upper bound of the lateral stress coefficient versus depth curve depends on lithology, while for the lower bound, the biaxial stress model ( $k = 1/3$ ) is a good approximation for all rock types. The relation between vertical and horizontal stresses for simple elastic earth models depend on the physical properties of the rock mass (isotropic, transversely isotropic, orthotropic). In the isotropic case with zero Poisson ratio, the application of vertical stress does not induce any horizontal strain and, therefore, no horizontal stress. The other end-member is a viscous fluid with the Poisson ratio,  $\nu = 0.5$  results in horizontal stresses equal to the applied vertical stress and Heim's rule is valid. Note that for undrained transformations in porous media (i.e., no fluid exchange), Poisson's ratio is also close to 0.5, although the formation is not a "viscous fluid". In between, typical Poisson ratios for rock are taken to be one-fourth (or one-third), indicating that the induced vertical stress is three times (or two times) the horizontal stress, respectively. For transversely isotropic rock, as is the case for sedimentary layered rock, the horizontal stresses may be as high as six times the vertical stress assuming the Poisson ratio perpendicular to bedding one-half Poisson ratio parallel to bedding (0.25). This anisotropic end-member scenario can result from a layered rock mass which was fractured during uplift in the Earth's

crust. Elastic behaviour during unloading (uplift), however, is much stiffer compared to the behaviour during loading (burial). Elastic rock properties determined in the laboratory are of utmost importance, and sometimes neglected when estimating stress magnitudes. Elastic rock behaviour, however, affects the development of in situ stresses. In the orthotropic case, three Poisson ratios of the rock have to be identified, which can be the result of three mutually perpendicular sets of discontinuities in the rock mass. From the Q-WSM data set follows that  $k_{max} = 9.5$  for crystalline and  $k_{max} = 7.5$  for sedimentary rock. These stress ratios are not distinguished according to the degree or type of rock anisotropy involved. A sub-classification of the Q-WSM data set according to rock anisotropy may be needed in future.

Dimensionless horizontal stresses were also used by Rummel et al. (1986) to interpret hydraulic fracturing data from 500 tests in 100 boreholes at 30 different geographical locations. The average of all data excluding results with abnormal stress-depth relations (Auburn, Auriat, Bad Creek, Fjällbacka) yields  $S_H/S_V = 0.15/z + 0.65$  and  $S_{H1}/S_V = 0.27/z + 0.98$  where the depth,  $z$  is the depth in kilometres. Note that it is difficult to compare stress ratios from Rummel et al. (1986) with stress ratios from Brown and Hoek (1978), since the latter used two envelopes of the lateral-stress coefficient, while the former treated minimum and maximum horizontal stress coefficients separately. Averaging the two envelopes in Brown and Hoek (1978) and calculating an average lateral stress coefficient, Brown and Hoek's 1978  $a$ -value of the spherical shell model turns out to be about four times the Rummel et al.'s (1986)  $a$ -value. In addition, Rummel et al.'s (1986) spherical shell off-set  $b$ -value turns out to be about twice the spherical shell  $b$ -value of Brown and Hoek's (1978) average value. Since it is the minimum horizontal stress component which is determined most reliably in hydraulic fracturing tests, the  $S_H/S_V$  ratio is more reliably than the  $S_{H1}/S_V$  ratio (cf. Fig. 7b). Note that the  $a$ -value from Rummel et al. (1986) is much closer to the  $a$ -value computed from the lower bound envelope of Brown and Hoek (1978).

Savage et al. (1992) modified the laterally constrained isotropic and homogeneous elastic half-space model under its own weight by allowing the crust to be subjected to small horizontal (tectonic) strains. They modified the findings for the case of transversely



isotropic and orthotropic rock material. Using Amadei et al.'s (1987) variation of the ratio of Young's modulus parallel and perpendicular to bedding from 1 to 3,—they computed horizontal stresses to vary between 0.13 and 0.93 times  $S_V$  for layered sedimentary rocks, which gives a maximum vertical stress value of  $\sim 8$  times the maximum horizontal stress value.

A mathematically different approach to interpret horizontal stress ratios in rock was given by Sen and Sadagah (2002). In their approach, the horizontal stress at a certain depth in the Earth's crust is assumed to have a common probability distribution function. Using Chebyshev inequality for random variables, they found an exponential relationship to predict the average stress ratio for a given depth which is contrary to the spherical shell relationship which has a parabolic form in general. Unfortunately, Sen and Sadagah (2002) when applying their probabilistic approach to Brown and Hoek's (1978) data set did not separate for different rock types, which is a pre-requisite for obtaining reliable data of stress estimation with depth.

In underground coal and limestone mines in eastern and mid-western US, Dolinar (2003) finds that unlike the vertical stress component, the horizontal stresses are not related to depth but the rock stiffness. This conclusion applies to the depth range investigated (<600 m) and to the geographic areas investigated. Kang et al. (2010) developed a portable small borehole hydraulic fracturing system for in situ stress measurements in Chinese underground coal mines. Data from 49 coal mines in six provinces indicate that the ratio of average horizontal stress and vertical stress ( $k = 0.5(S_h + S_H)/S_V$ ) can be expressed as  $k = 0.116/z + 0.7$ . The  $k$ -value decreases from  $k \sim 2.2$  at 200 m to  $k \sim 1$  at 1.4 km depth. This documents that the weak coal material has a similar  $k(z)$ -behaviour as demonstrated for the sedimentary rocks in Fig. 6b.

### 5.3 Stress Magnitudes, Q-WSM

There is still no final statement on whether stress increases linearly with depth. McGarr (1980) concluded that on average the maximum shear stress in rock increases linearly with depth in the upper 5 km of the Earth's crust. However, he makes a distinction between the maximum shear-stress gradient of crystalline (6.6 MPa/km) and sedimentary rock (3.8 MPa/km), with no suggestion of diminishing gradient at deeper levels. From Engelder's (1993) analysis of the

octahedral shear stress, the highest values came from crystalline rocks of the Appalachian Mountains (Moodus, Connecticut). The lowest values came from sedimentary rocks of the Michigan Basin. In general, stress magnitudes appear to increase with depth most rapidly in areas of active faulting (Moodus, San Andreas Fault). The least increase of stress magnitudes with depth is found in a stable continental interior (Canadian Shield, Michigan Basin, or Bavarian KTB site). This statement needs to be confirmed as more stress magnitudes are available in the new Q-WSM database.

When plotting stress magnitudes in 2D or 3D stress space (cf. Figs. 7, 8, 9), however, one needs to rely on different stress determination methods used for different stress components, and the assumptions involved in computing the maximum horizontal stress, which is the most difficult component of the stress tensor to accurately estimate from hydraulic methods (Zoback 2007). Instead of using hydraulic fracture data which are expensive, Bell (1990) recommended to use leak-off tests (LOT), which are often carried out while drilling exploratory wells. LOT pressures are likely to be higher than  $S_h$  affecting the surrounding rocks. For several wells drilled in offshore eastern Canada, Ervine and Bell (1987), however, concluded that the lower LOT pressures of the test data set were likely to be close to the fracture opening pressure and that, since the latter pressures were only marginally greater than the instantaneous shut-in pressures in many hydraulic fracture experiments, such LOT pressures gave good estimates of  $S_h$ . Bell (1990) used a lower bound to calculate the maximum horizontal stress,  $S_H = 2S_h + p_o$  where  $S_h$  is the measured formation LOT and  $p_o$  is the static formation pressure. There also exist analytical methods for determining horizontal stress bounds for wellbore data (Tan et al. 1993). For the case of sedimentary basins, overpressure mechanism is particular sensitive to stress magnitudes and vice versa, depending on the tectonic stress regime (Bell 1996).

In oil industry today, reliable methods determining in situ stress magnitudes are still based on the initiation, propagation and arrest of hydraulic (fluid-filled) fractures at depth. Methods commonly used are the traditional hydraulic fracturing (HF), leak-off tests (LOT) and extended leak-off tests (xLOT). LOT was originally developed in the oil industry to assess the "fracture gradient" of the formation (i.e., the

maximum borehole pressure that can be applied without mud loss) and to determine optimal drilling parameters such as mud density (Kunze and Steiger 1991). LOT and xLOT procedures have been successfully and widely used to estimate the minimum stress magnitudes (Addis et al. 1998; White et al. 2002; Yamamoto 2003), mainly for the practical purpose of determining borehole stability during drilling operations. However, these data can also be used for in situ stress information. For interpreting LOT results, the fracture pressure at the base of the casing is needed (Baumgärtner and Zoback 1989; De Bree and Walters 1989). LOT is a pumping pressure test analogous to HF with the difference that the HF is normally done in a section away from the drill hole bottom while the LOT is normally done at the very bottom of the drill hole and under the casing shoe. The difference in geometry between HF and LOT is likely to have an influence on the determination of the least principal stress. When fluid begins to enter the surrounding rock from the borehole (leak-off), the pressure build-up will deviate from the linear trend of the pressure–time curve. The point where this deviation occurs is known as leak-off pressure (LOP).

LOT can further run as xLOT to determine the fracture closure pressure (Gaarenstroom et al. 1993), which is measured after pumping is stopped and drilling fluids are no longer propping open any fractures. The fracture closure pressure represents the minimum stress magnitude (Yamamoto 2003), because the stress in the formation and the pressure of fluid that remains in the fractures have reached a state of mechanical equilibrium. The fracture closure pressure is determined by the intersection of the two tangents to the pressure–mud volume curve. White et al. (2002) collected high quality xLOT data and showed that both, the fracture closure pressure and the instantaneous shut-in pressure provide better estimates of the  $S_h$ -magnitude than LOP. The test can also be run multiple times (Yamamoto 2003), and off-shore (Lin et al. 2008) with the new riser-drilling vessel Chikyū which allows pressuring the entire casing string with drilling mud immediately after the casing is cemented in place. xLOT can provide data that are both, valuable and practical for estimating the magnitude of  $S_h$  (Nelson et al. 2007). A consistent fracture closure pressure in multiple tests gives greater confidence in  $S_h$  interpretation. To evaluate the pressure–volume curve during bleed-off (beyond the fracture closure

pressure), the flow-back volume is monitored in a flow meter. Raaen et al. (2006) identified pump-in/flow-back tests as to give a robust estimate of the minimum principal stress magnitude. Note, however, that calculation of  $S_h$  by using LOT and xLOT procedures depends on the assumption that a new fracture has been created in the plane perpendicular to the minimum principal stress by the pumping pressure and that pre-existing fractures, anisotropy and heterogeneity of the formation have no influence.

The minimum principal stress determined by xLOT is equivalent to the minimum principal horizontal stress ( $LOP = S_h$ ) in normal and strike-slip regimes, and the hydraulic fracture is induced in a vertical plane. In active thrust faulting belts, the minimum principal stress is equivalent to the vertical stress ( $LOP = S_v$ ), and the fracture is formed in a horizontal plane. In general, it is difficult to identify if the minimum principal stress is vertical or horizontal stress without mapping the actual hydraulic fracture induced. Another drawback of the xLOT procedure is that one cannot determine the maximum principal stress magnitude (Lin et al. 2008) which is also difficult to determine in standard HF (Ito et al. 2007). Recently, Couzens-Schultz and Chan (2010) gave an alternative interpretation of LOP. In active fault belts, they assume the LOT procedure to cause shear failure along pre-existing fractures (mode II fracture) instead of tensile opening (mode I fracture) as used previously, and come up with leak-off pressures in the range  $0.4 S_v < LOP < 0.7 S_v$ . The difference between LOT-mode I and LOT-mode II interpretation is most evident in compressive settings, when large differential stresses favour shear failure, but may be observed in all tectonic settings. If the mode II hypothesis is correct, this offers an opportunity to constrain also  $S_H$ -magnitudes in active thrust belts (Couzens-Schultz and Chan 2010).

Another approach of computing the maximum horizontal stress magnitude, is given by Zoback et al. (2003), when constructing possible stress states and  $S_H(S_h)$  polygons for different depth and faulting regimes. Combining the constraints on stress magnitudes obtained from frictional strength of the crust (Byerlee's law), measurements of  $S_h$  from LOT and observation of wellbore failure, they place constraints on the in situ state of stress. Assuming a friction coefficient of 0.6, Zoback et al. (2003) computed  $S_H$  from drilling-induced tensile fractures in the wall of a

vertical well by  $S_H = 3S_h + p_o$ . Further, Barton et al. (1988) used borehole breakout widths to estimate the  $S_H$  stress magnitude. To utilize these techniques, however, independent knowledge of pore pressure, the vertical stress, the least principal stress and rock strength are needed for estimation of  $S_H$  from breakout width. Recently, a fracture mechanics approach is used to determine stress magnitudes from the width and depth of borehole breakouts in Habanero granite from a geothermal field in Cooper Basin, Australia (Shen 2008). In summary, stress relations from published literature data points displayed in Fig. 7 may also reflect the assumptions needed in order to estimate  $S_H$  from measured  $S_h$  values. The future Q-WSM ranking system for stress magnitudes will account for this.

## 6 Conclusions

A new development of the World Stress Map (WSM) project is the global compilation of lithologic stress magnitudes versus depth in the Quantitative World Stress Map (Q-WSM) database. We draw the following conclusions from the WSM stress orientation database and first insights into Q-WSM stress magnitude database.

- (1) For rock mechanics and rock engineering sized volumes, it is recommended to use the WSM quality ranking system for stress orientations with A–C data quality (accuracy  $\pm 25^\circ$ ), and to rely on the three most important techniques like hydraulic methods (hydraulic fracturing, (extended) leak-off tests), borehole breakouts, drilling induced tensile fractures and overcoring methods.
- (2) In creating stress orientation maps from WSM database with A–C data quality, it is recommended to display both, measured-discrete orientation maps, and smoothed-computed stress orientation maps with adequate smoothers (number of data records, search radius) in order to improve fluctuation in data while preserving larger-scale stress orientation trends.
- (3) Using the Q-WSM database, it is possible to display stress ratios and lateral stress coefficients versus depth, faulting regime and rock type. This will be of valuable information, when initial conditions for in situ stress reservoir models are required, or rock engineering underground excavations and drilling are planned at a specific site. Each material has its own characteristic stress ratio-depth variability.
- (4) Plotting Q-WSM stress magnitude data in 2D and 3D stress space is helpful in identifying generic trends of the stress magnitudes for different rock types and faulting regimes.
- (5) To account for specific downhole stress states in Q-WSM, stress magnitudes, pore pressure and elastic rock properties as well as rock fracture and friction strength values from true-triaxial testing are required (Mogi 2007). A second quality ranking system for stress magnitudes is under way.

**Acknowledgments** We would like to thank two anonymous reviewers for their valuable input. We appreciate the thorough reading from the oil industry perspective (reviewer 1), and comments from the rock mechanics and rock engineering perspective (reviewer 2). The first author was supported by the European Union funded project GEISER (Geothermal Engineering Integrating Mitigation of Induced Seismicity in Reservoirs, Grant agreement no.: 241321-2). He would like to thank Ernst Huenges and David Bruhn (both GFZ, Section 4.1 Reservoir Technology).

## References

- Aadnoy BS, Hansen AK (2005) Bounds on in situ stress magnitudes improve wellbore stability analyses. *Soc Petroleum Eng SPE J* 10(2):115–120
- Addis MA, Hanssen TH, Yassir N, Willoughby DR, Enever J (1998) A comparison of leak-off test and extended leak-off test data for stress estimation. SOE/IRSM 47235. In: Proceedings of ISRM EUROCK98, vol 2, Trondheim, Norway, pp 131–140
- Amadei BS, Stephansson O (1997) Rock stress and its measurements. Chapman and Hall, London
- Amadei BS, Savage WZ, Swolfs HS (1987) Gravitational stresses in anisotropic rock masses. *Int J Rock Mech Min Sci Geomech Abstr* 24:5–14
- Angelier J (2002) Inversion of earthquake focal mechanism to obtain the seismotectonic stress IV—a new method free of choice among nodal planes. *Geophys J Int* 150:588–609
- Aydan Ö (1995) The stress state of the Earth and the Earth's crust due to gravitational pull. In: Daemen JJK, Schulz RA (eds) Proceedings of the 35th US symposium on rock mechanics, Lake Tahoe. AA Balkema, Rotterdam, pp 237–243
- Barton CA, Zoback MD, Burns KL (1988) In situ stress orientation and magnitude at the Fenton Hill geothermal site, New Mexico, determined from borehole breakouts. *Geophys Res Lett* 15(5):467–470

- Baumgärtner J, Zoback MD (1989) Interpretation of hydraulic fracturing pressure-time records using interactive analysis methods. *Int J Rock Mech Min Sci* 26:461–470
- Bell JS (1990) Investigating stress regimes in sedimentary basins using information from oil industry wireline logs and drilling records. In: Hurst A, Lovell MA, Morton AC (eds) *Geological applications of wireline logs*. Geological Society Special Publications No. 48, London, pp 305–325
- Bell JS (1996) Petro geoscience 2. In situ stresses in sedimentary rocks (part 2): applications of stress measurements. *Geosci Can* 23(3):135–153
- Bell JS, Gough DI (1979) Northeast-southwest compressive stress in Alberta: evidence from oil wells. *Earth Planet Sci Lett* 45:475–482
- Bieniawski ZT (1984) *Rock mechanics design in mining and tunnelling*. AA Balkema, Rotterdam
- Bird P (2003) An updated digital model for plate boundaries. *Geochem Geophys Geosyst* 4:1027–1079
- Brown ET, Hoek E (1978) Trends in relationships between measured in situ stresses and depth. *Int J Rock Mech Min Sci Geomech Abstr* 15:211–215
- Cannolly P, Cosgrove J (1999) Prediction of static and dynamic fluid pathways within and around dilational jogs. In: McCaffrey KJW, Lonergan L, Wilkinson JJ (eds) *Fractures, fluid flow and mineralization*, vol 155. Special Publications: Geological Society, London, pp 105–121
- Cornet FH, Burlet D (1992) Stress field determination in France by hydraulic tests in boreholes. *J Geophys Res* 97:11829–11849
- Couzens-Schultz BA, Chan AW (2010) Stress determination in active thrust belts: an alternative leak-off pressure interpretation. *J Struct Geol* 32:1061–1069
- De Bree P, Walters JV (1989) Micro/Minifrac test procedures and interpretation for in situ stress determination. *Int J Rock Mech Min Sci Geomech Abstr* 26:515–521
- DeMets C, Gordon RG, Argus DF, Stein S (1994) Effect of recent revisions to the geomagnetic reversal time scale on estimates of current plate motions. *Geophys Res Lett* 21(20):2191–2194
- DeMets C, Gordon RG, Argus DF (2010) Geologically current plate motions. *Geophys J Int* 181:425–478
- Dolinar DR (2003) Variation of horizontal stresses and strains in mines in bedded deposits in the eastern and midwestern United States. In: 22nd international conference on ground control in mining, society for mining, metallurgy and exploration (SME), chapter 26 geotechnical planning, p 8
- Engelder T (1993) *Stress regimes in the lithosphere*. Princeton University Press, Princeton
- Ervine WB, Bell JS (1987) Subsurface in situ stress magnitudes from oil-well drilling records: an example from the Venture area, offshore eastern Canada. *Can J Earth Sci* 24(9):1748–1759
- Fuchs K, Müller B (2001) World stress map of the Earth: a key to tectonic processes and technological applications. *Naturwissenschaften* 88:357–371
- Gaarenstroom L, Tromp RAJ, de Jong MC, Brandenburg MA (1993) Overpressures in the Central North Sea: implications for trap integrity and drilling safety. In: Parker JD (ed) *Geology of Northwest Europe*, Proceedings of the 4th conference, pp 1305–1313
- Gough DI, Gough WI (1987) Stress near the surface of the Earth. *Annu Rev Earth Planet Sci* 15:545–566
- Grünthal G, Stromeyer D (1994) The recent crustal stress field in Central Europe sensu lato and its quantitative modelling. *Geologie en Mijnbouw* 73:173–180
- Haimson BC (1975) The state of stress in the earth's crust. *Rev Geophys Space Phys* 13:350–352
- Haimson BC (1978) The hydrofracturing stress measuring method and recent field results. *Int J Rock Mech Min Sci Geomech Abstr* 15:167–178
- Haimson BC (2007) Micromechanisms of borehole instability leading to breakouts in rock. *Int J Rock Mech Min Sci Geomech Abstr* 44:157–173
- Haimson BC, Cornet FC (2003) ISRM suggested method for rock stress estimation—part 3: Hydraulic fracturing (HF) and/or hydraulic testing of pre-existing fractures (HTPF). *Int J Rock Mech Min Sci* 40:1011–1020
- Haimson BC, Lee CF (1995) Estimating in situ stress conditions from borehole breakouts and core diskings. In: Proceedings 8th ISRM congress, international workshop on rock stress measurement at great depth, Tokyo, Japan. Balkema, Rotterdam, pp 19–24
- Hakala M, Kuula H, Hudson JA (2007) Estimating the transversely isotropic elastic intact rock properties for in situ stress measurement data reduction: a case study of the Olkiluoto mica gneiss, Finland. *Int J Rock Mech Min Sci* 44:14–46
- Hast N (1969) The state of stress in the upper part of the Earth's crust. *Tectonophysics* 8:169–211
- Heidbach O, Reinecker J, Tingay M, Müller B, Sperner B, Fuchs K, Wenzel F (2007) Plate boundary forces are not enough: Second- and third-order stress patterns highlighted in the World Stress Map database. *Tectonics* 26:TC6014. doi: 10.1029/2007TC002133
- Heidbach O, Tingay M, Barth A, Reinecker J, Kurfeß D, Müller B (2008) The 2008 release of the World Stress Map. Available online: <http://www.world-stress-map.org>
- Heidbach O, Tingay M, Barth A, Reinecker J, Kurfeß D, Müller B (2010) Global crustal stress pattern based on the 2008 World Stress Map database release. *Tectonophysics* 482:3–15
- Henk A (2008) Perspectives of geomechanical reservoir models—why stress is important. *Eur Mag* 4:1–5
- Hergert T, Heidbach O (2011) Geomechanical model of the Marmara Sea region—II. 3-D contemporary background stress field. *Geophys J Int* 185(3):1090–1102
- Herget G (1974) Ground stress determinations in Canada. *Rock Mech* 6:53–74
- Herget G (1987) Stress assumptions for underground excavations in the Canadian shield. *Int J Rock Mech Min Sci Geomech Abstr* 24:95–97
- Hickman SH (1991) Stress in the lithosphere and the strength of active faults. *Rev Geophys* 29:759–775
- Hopkins CW (1997) The importance of in situ-stress profiles in hydraulic-fracturing applications. *Soc Petroleum Eng SPE* 38458:944–948
- Hubbert KM, Willis DG (1957) Mechanics of hydraulic fracturing. *Petroleum Trans AIME T.P.* 4597, 210:153–166
- Hudson JA, Harrison JP (2000) *Engineering rock mechanics*. Elsevier Science Ltd, Kidlington



- Hudson JA, Cornet FH, Christiansson R (2003) ISRM suggested methods for rock stress estimation—part I: strategy for rock stress estimation. *Int J Rock Mech Min Sci* 40(7–8): 991–998
- Isra J, Galybin AN (2010) Stress trajectories element method for stress determination from discrete data on principal directions. *Eng Anal Boundary Elem* 34:423–432
- Ito T, Omura K, Ito H (2007) BABHY—a new strategy of hydrofracturing for deep stress measurements. *Sci Drill Special Issue* 1:113–116
- Kang H, Zhang X, Si L, Wu Y, Gao F (2010) In situ stress measurements and stress distribution characteristics in underground coal mines in China. *Eng Geol* 116:333–345
- Kunze KR, Steiger RP (1991) Extended leak-off tests to measure in situ stress during drilling. In: Roegiers J-C (ed) *Rock mechanics as a multidisciplinary science*. Balkema, Rotterdam, pp 33–44
- Li Y, Schmitt DR (1998) Drilling-induced core fractures and in situ stress. *J Geophys Res* 103(B3):5225–5239
- Lin W, Yamamoto K, Ito H, Masago H, Kawamura Y (2008) Estimation of the minimum principal stress from extended leak-off tests onboard the Chikyu drilling vessel and suggestions for future test procedures. *Sci Drill* 6:43–47
- Lin W, Yeh C-H, Hung J-H, Haimson B, Hirono T (2010) Localized rotation of principal stress around faults and fractures determined from borehole breakouts in hole B of the Taiwan Chelungpu-fault Drilling Project (TCDP). *Tectonophysics* 482:82–91
- Ljunggren C, Chang Y, Janson T, Christiansson R (2003) An overview of rock stress measurement methods. *Int J Rock Mech Min Sci* 40:975–989
- Lund B, Zoback MD (1999) Orientation and magnitude of in situ stress to 6.5 km depth in the Baltic Shield. *Int J Rock Mech Min Sci* 36:169–190
- McCutchen WR (1982) Some elements of a theory for in situ stress. *Int J Rock Mech Min Sci Geomech Abstr* 19:201–203
- McGarr A (1980) Some constraints on levels of shear stress in the crust from observation and theory. *J Geophys Res* 85:6231–6238
- McGarr A, Gay NC (1978) State of stress in the Earth's crust. *Ann Rev Earth Plan Sci* 6:405–436
- Moeck I, Backers T (2011) Fault reactivation potential as a critical factor during reservoir stimulation. *First Break* 29:73–80
- Mogi K (2007) *Experimental rock mechanics*. Geomechanics research series, vol 3. Taylor & Francis Group, London
- Morris A, Ferrill DA, Henderson DB (1996) Slip tendency analysis and fault reactivation. *Geology* 24:275–278
- Müller B, Zoback ML, Fuchs K, Mastin L, Gregersen S, Pavoni N, Stephansson O, Ljunggren C (1992) Regional patterns of tectonic stress in Europe. *J Geophys Res* 97:11783–11803
- Müller B, Wehrle V, Hettel S, Sperner B, Fuchs F (2003) A new method for smoothing oriented data and its application to stress data. In: M Ameen (ed) *Fracture and in situ stress characterization of hydrocarbon reservoirs*, vol 209. Special Publication: Geological Society, London, pp 107–126
- Nelson EJ, Chipperfield ST, Hillis RR, Gilbert J, McGown J, Mildren SD (2007) The relationship between closure pressures from fluid injection tests and the minimum principal stress in strong rocks. *Int J Rock Mech Min Sci* 44:787–801
- Raaen AM, Horsrud P, Kjørhold H, Okland D (2006) Improved routine estimation of the minimum horizontal stress component from extended leak-off tests. *Int J Rock Mech Min Sci* 43:37–48
- Ranalli G, Chandler TE (1975) The stress field in the upper crust as determined from in situ measurements. *geol. Rundschau* 64:653–674
- Rasouli V, Pallikathakathil ZJ, Mawuli E (2011) The influence of perturbed stresses near faults on drilling strategy: a case study in Blacktip field, North Australia. *J Petr Sci Eng* 76:37–50
- Roth F, Fleckenstein P (2001) Stress orientations found in North-east Germany differ from the West European trend. *Terra Nova* 13:289–296
- Rummel F (1979) Stresses in the upper crust as derived from in situ stress measurements—a review. *Progress in earthquake prediction research*. Vieweg, Braunschweig, pp 391–405
- Rummel F (1986) Stresses and tectonics of the upper continental crust, a review. In: Stephansson O (ed) *Rock stress and rock stress measurements*. Centek Publishers, Lulea, pp 177–186
- Rummel F (ed) (2005) *Rock mechanics with emphasis on stress*. AA Balkema Publishers, Leiden
- Rummel F, Möhring-Erdmann G, Baumgärtner J (1986) Stress constraints and hydro-fracturing stress data for the continental crust. *PAGEOPH* 124(4/5):875–895
- Sano O, Ito H, Hirata A, Mizuta Y (2005) Review of methods of measuring stress and its variations. *Bull Earthq Res Inst Univ Tokyo* 80:87–103
- Savage WZ, Swolfs HS, Amadei B (1992) On the state of stress in the near surface of the Earth's crust. *PAGEOPH* 138: 207–228
- Sbar ML, Sykes LR (1973) Contemporary compressive stress and seismicity in eastern North America, an example of intraplate tectonics. *Geol Soc Am Bull* 84:1861–1882
- Scholz CH (2002) *The mechanics of earthquakes and faulting*, 2nd edn. Cambridge University Press, New York
- Sen Z, Sadagah BH (2002) Probabilistic horizontal stress ratios in rock. *Math Geol* 34(7):845–855
- Shen B (2008) Borehole breakouts and in situ stresses In: Potvin Y, Carter J, Dyskin A, Jeffrey J (eds) *SHIRMS 2008*. Australian Centre for Geomechanics, Perth, pp 407–418
- Sheorey PR (1994) A theory for in situ stresses in isotropic and transversely isotropic rock. *Int J Rock Mech Min Sci Geomech Abstr* 31:23–34
- Sperner B, Müller B, Heidbach O, Delvaux D, Reinecker J, Fuchs K (2003) Tectonic stress in the Earth's crust: advances in the World Stress Map project. In: DA Nieuwland (ed) *New insights in structural interpretation and modelling*. Geological Society, London, Spec Pub Ser 212, pp 101–116
- Steinberger B, Torsvik TH (2008) Absolute plate motions and true polar wander in the absence of hotspot tracks. *Nature* 452:620–623
- Stephansson O, Särkkä P, Myrvang A (1986) State of stress in Fennoscandia. In: *Proceedings international symposium on rock stress and rock stress measurements*, Stockholm. Centek Publisher, Lulea, pp 21–32

- Sykes LR, Sbar ML (1973) Intraplate earthquakes, lithospheric stresses and the driving mechanism of plate tectonics. *Nature* 245:298–302
- Tan CP, Willoughby DR, Zhou S, Hillis RR (1993) An analytical method for determining horizontal stress bounds from wellbore data. *Int J Rock Mech Min Sci Geomech Abstr* 30(7):1103–1109
- Thiercelin MJ, Plumb RA (1994) Core-based prediction of lithologic stress contrasts in East Texas formations. *SPE Form Eval Pap SPE* 21847:251–258
- Tingay M, Hillis RR, Morley CK, Swarbrick E, Drake SJ (2005a) Present-day stress orientation in Brunei: a snapshot of ‘prograding tectonic’ in a Tertiary delta. *J Geol Soc Lond* 162:39–49
- Tingay M, Müller B, Reinecker J, Heidbach O, Wenzel F, Fleckenstein P (2005b) Understanding tectonic stress in the oil patch: The World Stress Map Project. *The Leading Edge*, pp 1276–1282
- Tingay MRP, Hillis RR, Morley CK, King RC, Swarbrick ER, Damit AR (2009) Present-day stress and neotectonics of brunei: implications for petroleum exploration and production. *AAPG Bull* 93:75–100
- Tonon F, Amadei B (2003) Stresses in anisotropic rock masses: an engineering perspective building on geological knowledge. *Int J Rock Mech Min Sci* 40:1099–1120
- van Heerden WL (1976) Practical application of the CSIR triaxial stress cell for rock stress measurements. In: *Proceedings ISRM symposium on investigation of stress in rock, advances in stress measurements*. The Institution of Engineers, Sydney, Australia, pp 1–6
- Voight B (1969) Evolution of North Atlantic Ocean: relevance of rock-pressure measurements North Atlantic—geology and continental drift. *AAPG Mem* 12:955–962. *Am Assoc Petroleum Geologists*
- White AJ, Traugott MO, Swarbrick RE (2002) The use of leak-off tests as a means of predicting minimum in situ stresses. *Petroleum Geosci* 8:189–193
- Wileveau Y, Cornet FH, Desroches J, Blümling P (2007) Complete in situ stress determination in the argillite sedimentary formation. *Phys Chem Earth* 32:866–878
- Yamamoto M (2003) Implementation of the extended leak-off test in deep wells in Japan. In: Sugawara K (ed) *Proceedings of 3rd international symposium on rock stress*. Balkema, Rotterdam, pp 225–229
- Zang A, Stephansson O (2010) *Stress field of the Earth’s crust*. Springer Science + Business Media, Dordrecht
- Zoback ML (1992) First- and second-order patterns of stress in the lithosphere: the World Stress Map project. *J Geophys Res* 97:11,703–11,728
- Zoback MD (2007) *Reservoir geomechanics*. Cambridge University Press, New York
- Zoback ML, Zoback MD (1980) State of stress in conterminous United States. *J Geophys Res* 85:6113–6156
- Zoback ML, Zoback MD (1989) Tectonic stress field of the conterminous United States. In: Pakiser LC, Mooney WD (eds) *Geophysical framework of the continental united states*, Boulder, Colorado, *Geol Soc Am Mem* 172:523–539
- Zoback MD, Zoback ML (1991) Tectonic stress field of North America and relative plate motions. In: Slemmons DB, Engdahl ER, Zoback MD, Blackwell DD (eds) *Neotectonics of North America, decade map, vol I.*, Geological Society of America/Boulder, Colorado, pp 339–366
- Zoback ML, Zoback MD, Adams J, Assumpcao M, Bell S, Bergman EA, Blümling P, Brereton NR, Denham D, Ding J, Fuchs K, Gay N, Gregersen S, Gupta HK, Gvishiani A, Jacob K, Klein R, Knoll P, Magee M, Mercier JL, Mueller BC, Paquin C, Rajendran K, Stephansson O, Suarez G, Suter M, Udias A, Xu ZH, Zhizhin M (1989) Global patterns of tectonic stress. *Rev Article Nat* 341:291–298
- Zoback MD, Barton CA, Brudy M, Castillo DA, Finkbeiner T, Grollimund BR, Moos DB, Peka P, Ward CD, Wiprut DJ (2003) Determination of stress orientation and magnitude in deep wells. *Int J Rock Mech Min Sci* 40:1049–1076